

# Compatibilizing Effect of Functionalized Polyphosphazene on the Properties of Poly(phenylene oxide)/Vectra A Blend System

S. Bose,<sup>1,2</sup> C. K. Das,<sup>1</sup> A. K. Saxena,<sup>3</sup> A. Ranjan<sup>3</sup>

<sup>1</sup>Materials Science Centre, IIT, Kharagpur, West Bengal 721302, India

<sup>2</sup>Department of Polymer and Nano Engineering, Chonbuk National University, Jeonju, Jeonbuk 561-756, South Korea

<sup>3</sup>DMSRDE, Kanpur, Uttar Pradesh, India

Received 18 December 2009; accepted 1 June 2010

DOI 10.1002/app.32912

Published online 23 August 2010 in Wiley Online Library (wileyonlinelibrary.com).

**ABSTRACT:** The effect of functionalized polyphosphazene on the thermal, rheological, and morphological properties of PPO (poly(phenylene oxide))/liquid crystalline polymer (Vectra A) blend has been investigated by means of the capillary rheometry, mechanical testing, and scanning electron microscopy (SEM) in this study. The rheological measurements show that compatibilized blends exhibit substantial rise in viscosity in comparison to uncompatibilized blend especially pronounced at lower shear rates which results in improved interfacial adhesion. DMA study highlights that polyphosphazene could be used as an effective compatibilizer for the concerned blend system. SEM study reveals fine fibrillation of liquid crys-

talline polymers in presence of compatibilizer and the fibers are oriented in the direction of flow field. The mechanical properties of the ternary blends are increased when a proper amount of polyphosphazene is added. This is attributed to fine strand generation induced via the addition of polyphosphazene. Enhanced adhesion at the interface invokes better elongation in the ternary blends. However, mechanical properties deteriorate considerably when polyphosphazene content is 5 wt %. © 2010 Wiley Periodicals, Inc. *J Appl Polym Sci* 119: 1914–1922, 2011

**Key words:** poly(phenylene oxide); adhesion; compatibilization

## INTRODUCTION

Recently, polyblends containing thermotropic liquid crystalline polymers (TLCPs) and thermoplastics have attracted much research attention.<sup>1–8</sup> Interest arises from two major advantages of blending LCPs with engineering thermoplastics. First, the LCPs can exhibit low melt viscosity, hence the addition of a small amount of LCPs to thermoplastics may result in a considerable reduction in the blend melt viscosity thereby improving the processability of engineering plastics.<sup>9–11</sup> Second, the LCPs have a more rigid molecular structure and they generally exhibit a high degree of orientation in melt under the conditions of shear and extension during processing.<sup>12</sup>

However, lack of miscibility between TLCPs and thermoplastics leads to poor dispersion and thereby degrades mechanical properties of the blends.<sup>13–15</sup> This lacuna needs to be addressed in such a way so that we can achieve polymer blends having superior mechanical, thermal, and morphological properties.

One way to solve the aforementioned problem is by the use of compatibilizer. O'donnell and Baird<sup>16</sup> have studied the effect of maleic anhydride grafted polypropylene (MAP) on the morphology and mechanical properties of PP/LCP blends. The tensile modulus of the PP/LC poly(ester amide) blend showed a 19% increase as the amount of MAP was increased above 5 wt %. The addition of MAP to PP/LCP blends reveals increased dispersion of the LCP phase and reduced interfacial tension between the concerned phases.

Poly(phenylene oxide) (PPO) can exhibit low moisture absorption, high mechanical properties, and excellent dimensional stability. However, the main disadvantageous feature of PPO is their high melt viscosity. Using HIPS the processability of PPO can be improved, but transparency can't be achieved and another problem associated with HIPS is that it absorbs moisture readily. LCP can eliminate the shortcomings offered by HIPS. Now to reduce the melt viscosity blending of PPO with LCP is very essential. In this study, we are dealing with PPO/TLCP blend in presence of polyphosphazene, used as an effective compatibilizer for the concerned blend system. Compatibilization of PPO/LCP blends by semi-interpenetrating liquid crystalline polymer networks has been investigated by Zhao et al.<sup>17</sup>

Correspondence to: S. Bose (bose\_saswata@yahoo.co.in or saswataboseiit@gmail.com).

According to Zhao et al., the bending strength and the Izod impact strength of the compatibilized sample with 5% semi-ILCPN increase more than two and four times as compared with the uncompatibilized PPO/LCP blend system, respectively. Chiang and Chang<sup>18</sup> showed the styrene-glycidyl methacrylate (SG) copolymer has been demonstrated to be an effective reactive compatibilizer to improve the processability, heat deflection temperature, and mechanical properties of PPO/LCP blends. However, the effectiveness of polyphosphazene elastomer on the thermal, mechanical, and morphological properties of PPO/LCP blend is yet to be explored.

In this study, polyphosphazene has been used to compatibilize PPO/LCP (Vectra A950, hereafter referred as VA) blends. The processability, thermal behavior, morphology and interfacial property of PPO/LCP blends in presence of compatibilizer are studied. On the basis of aforementioned researches, the main goal of this study is to interpret the effect of compatibilization of polyphosphazene for PPO/VA blends.

## EXPERIMENTAL

This section briefly introduces the materials used in this study for carrying out comprehensive experimental investigations followed by brief discussions about the characterization techniques adopted for analysis of the thermal, rheological, and morphological properties of PPO/LCP and PPO/LCP/polyphosphazene blend systems.

### Materials used

1. Poly(phenylene oxide) (PPO) (General Electric), molecular weight of repeat unit is 120.15 g/mol and glass transition temperature of about 212°C.
2. Thermotropic liquid crystalline polymer was Vectra A950, supplied by Ticona, USA. The LCP has the comonomer composition of 75 mole % of hydroxybenzoic acid (HBA) and 25 mol % of hydroxynaphthoic acid (HNA).
3. Polyphosphazenes (having  $-\text{OPhCH}=\text{CH}_2$ , side group), which was used in this study as compatibilizer, was obtained from DMSRDE, Kanpur, India.

### Preparation of PPO/LCP/polyphosphazene composite

The pellets of the PPO and Vectra-A950 were dried in a vacuum oven at 100°C for 12 h before use to remove the last traces of water.<sup>19,20</sup> Then dry pellets of PPO, Vectra-A950, and polyphosphazenes were

melt-blended in a twin-screw extruder, which was equipped with a screw of 19 mm in diameter, compression ratio (3 : 1), and  $L/D$  ratio of 25. The extrusion temperature of the feeding zone/transporting zone/melting zone were set as 160/250/300°C at a rotor speed of 80 rpm. The extrudates were subsequently pelletized. Then, the pelletized composites were compression molded under constant pressure of about 15 MPa at 300°C for 10 min. Compounding formulation is given in Table I.

### Characterization

In this section, a brief detail of the adopted characterization techniques has been put forward.

#### Torque measurement

The melting torques of the pure PPO, VA, and their blends were determined with a Brabender Plasticorder at a capacity of 50 cc and operated at 285°C and 30 rpm for 10 min.

#### Rheological analysis

Rheology measurements were carried out on Ceast capillary rheometer Model. Samples were loaded in pellet form at 300°C. Approximately 15 min was required for the system to reach thermal equilibrium. Diameter of the die was 0.5 mm. Measurements were carried out over a shear rate range of 50 to 2000/s.

#### Thermogravimetric analysis

Thermogravimetric analysis (TGA) was conducted in air using a Dupont TGA-2100 thermal analyzer at 50–650°C, with a heating rate of 10°C/min.

#### Dynamic mechanical thermal analysis

Dynamic mechanical analysis was performed in a TA instrument DMA 2980 dynamic mechanical analyzer with a frequency of 1 Hz and a heating rate of 2°C/min. The temperature dependence of storage modulus  $E'$ , loss modulus  $E''$ , and loss tangent ( $\tan \delta$ ) was measured from 50 to 200°C. The measurements were carried out in tensile mode.

#### Heat deflection temperature

The heat deflection temperature (HDT) is the temperature at which a polymer or plastic sample deforms under a specified load. This property of a given plastic material is applied in many aspects of product design, engineering, and manufacture of products using thermoplastic components. Heat

**TABLE I**  
**Compounding Formulation**

Sample code	PPO (wt %)	VA (wt %)	Polyphosphazene
P	100		
P1	75	25	
P2	75	22.5	2.5
P3	75	20	5

deflection temperature measurements (HDT) were carried out according to ASTM-D648, standard using 66 psi loading at a heating rate of 2°C/min.

#### Fourier transform infrared spectroscopy

Fourier transform infrared (FTIR) spectroscopic study was carried out using a NEXUS 870 FT-IR (Thermo Nicolet) in a humidity-free atmosphere at room temperature from 500 to 2000/cm. The experiment was carried out taking compression molded thin films in absorbance mode with a 4/cm resolution for 64 scans.

#### X-ray diffraction

X-ray diffraction (XRD) study was carried out using PW 1840 X-ray diffractometer with Cu-K $\alpha$ -targets at 2 mm slits at a scanning rate of 0.050 2 $\theta$ /s, chart speed 10 mm/2 $\theta$ , range 5000 c/s, operated at 40 kV, 20 mA, to get an explicit idea of the relative crystallinity of the composites. The area under the X-ray diffractogram was determined in arbitrary units. The percentage of crystallinity,  $\chi_c$ , was measured using the following relationship:

$$\chi_c = I_c / (I_a + I_c) \times 100$$

where,  $I_a$  and  $I_c$  are the integrated intensity of the amorphous and crystalline region, respectively.

The crystallite sizes ( $P$ ) and the interplanar distance ( $d$ ) were calculated as follows:

$$P = K\lambda / \beta \cos \theta$$

$$d = \lambda / 2 \sin \theta$$

where,  $\beta$  is the half height width (in radian) of the crystalline peak and  $\lambda$  is the wave length of the X-ray radiation (1.5404 for Cu) and  $K$  is the Scherrer constant taken as 0.9.

#### Mechanical testing

Tensile measurement of the blends was done using a HOUNSFIELD (modelH10KS) at constant temperature and humidity. A gauge length of 35 mm and a crosshead speed of 5 mm/min were used.

#### Scanning electron microscopy

Scanning electron microscopy (SEM) study was carried out in VEGA TESCAN//LSU. The cryo-fractured samples were coated with thin gold.

## RESULTS AND DISCUSSION

#### Torque measurements

Variation of mixing torque as a function of mixing time has been shown in Figure 1. From Figure 1, it is evident that the torque values of both pure PPO and pure LCP decreases gradually with mixing time which may be due to the slight hydrolytic degradation which has been effected by moisture. However, incorporation of VA leads to decrease the melt torque of pure PPO corroborating the incompatibility between PPO and dispersed LCP phase. In presence of polyphosphazene elastomer, mixing torque increases steadily with mixing time revealing the possible interaction of phenolic-OH end group of PPO with LCP and polyphosphazene leading to improved interfacial adhesion.

#### Flow behavior

The flow properties of pure PPO (P), VA, and blended materials (P1, P2, and P3) are investigated at 300°C using a capillary rheometer. The viscosity–shear rate relationship for the pure PPO and the blends are exhibited in Figure 2. The viscosities of the binary and the ternary blends are lower than those of the neat polymers, indicating a synergistic effect of VA in reducing the melt viscosity and also signifying its great ability as a processing aid. The compatibilized blends exhibit in substantial rise in viscosity in comparison to uncompatibilized blend especially pronounced at lower shear rates which

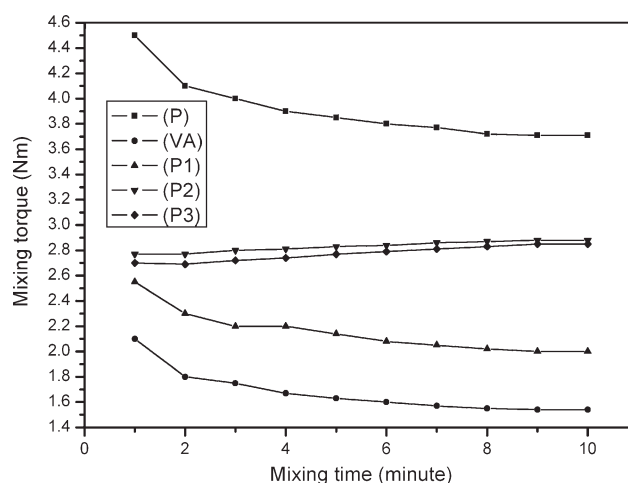


**Figure 1** Plot of mixing torque versus mixing time.

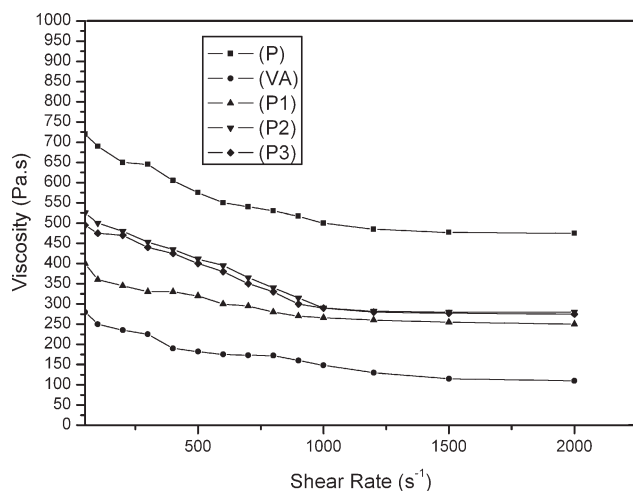


**Figure 2** Viscosity versus shear rate pattern at 300°C.

results in improved interfacial adhesion. The rise in viscosity is probably due to following reasons:

1. Phase structural transformation,
2. Increase in molecular weight through grafting reaction,
3. Increase of the interfacial friction of the compatibilized blend, and
4. Increase in the contact area between the PPO and the dispersed LCP phase in presence of polyphosphazene.

However, viscosities of the polyphosphazene-compatibilized or uncompatibilized blend become almost similar in magnitude at high shear rate region and showing a Newtonian behavior of flow. This phenomenon is presumably due to shear thinning effect which takes place due to drop off in the LCP fibrils-matrix collision caused by alignment of the LCP fibrils along the direction of flow at high shear rates.

### Thermogravimetric analysis

Thermal stability of the uncompatibilized and compatibilized PPO/VA blends is exhibited in Figure 3. Onset degradation temperature of pure PPO appears at 411°C, whereas with the addition of VA, a significant decrease in thermal stability is observed (370°C) which is probably due to structural transformation caused by VA. Again in presence of 2.5 wt % polyphosphazene, 8°C increment of onset degradation temperature is observed. The superior thermal stability can be apparently attributed to the following:

1. Favorable effects of polar and the bulky pendant group of polyphosphazene, and
2. Structural reorganization of PPO matrix demonstrating that the polyphosphazene used as a compatibilizer strengthens the interaction between the

organic polymer matrix phase and dispersed VA phase.

However, in presence of 5 wt % polyphosphazene, thermal stability is decreased in comparison to PPO/VA/2.5 wt % polyphosphazene blend system corroborating coagulation or flocculation of the dispersed VA phase.

### Dynamic mechanical thermal analysis

DMA methods have been extensively used for the analysis of the phase behavior of the polymer blends. This technique is usually more sensitive than DSC for detecting unclear transitions in some semicrystalline polymers including most of TLCPs. The storage modulus ( $E'$ ) as a function of temperature is graphically represented in Figure 4(a) and the corresponding observations are summarized in Table II. From Figure 4(a), it has been observed that prior to glass transition temperature ( $T_g$ ) compatibilized blend systems render better stiffness than the uncompatibilized one indicating an improvement of the compatibility of PPO/LCP blend system in presence of polyphosphazene. Therefore, interfacial interactions are being facilitated by allowing better stress transfer from matrix phase to dispersed LCP phase.

The variation of loss tangent ( $\tan \delta$ ) as a function of temperature is shown in Figure 4(b), and the relevant data are summed up in Table III.  $T_g$  for pure PPO appears at 212°C<sup>21,22</sup> and VA has a low, broad transition peak at 117°C. For the PPO/VA blend, two loss peaks were detected; one is corresponding to VA phase at about 115°C and other corresponding to PPO phase at about 183°C. The shifting of glass transition temperature is probably due to polar interaction between LCP and PPO. But, phase separation is evident (appearance of two distinct  $T_g$ ) in

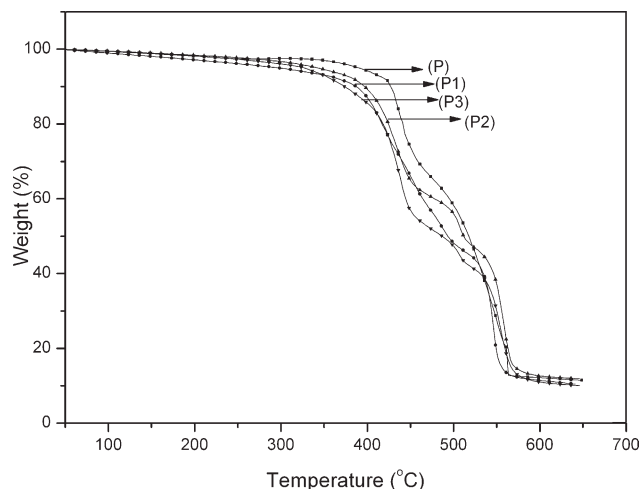


**Figure 3** TGA thermograms of pure PPO (P), PPO/VA (P1), and PPO/VA/polyphosphazenes (P2 and P3).

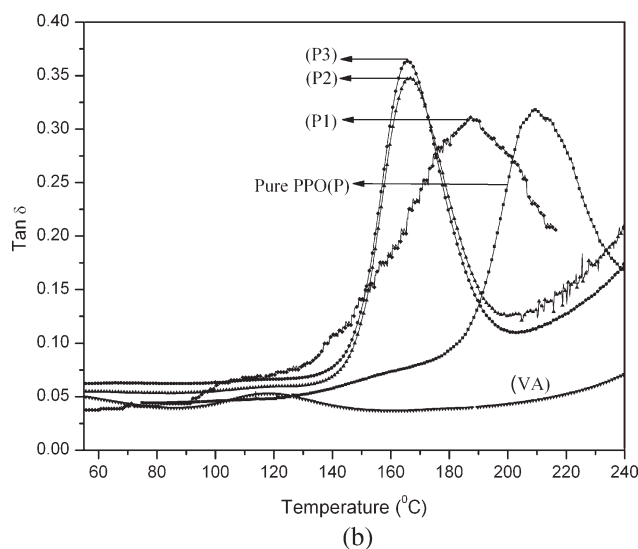
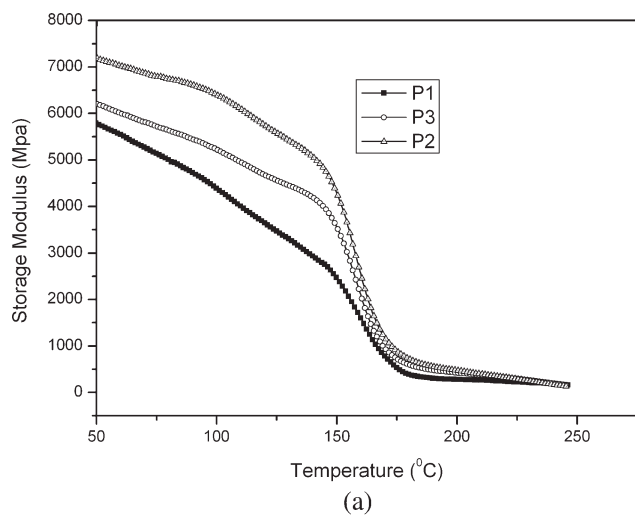


**Figure 4** (a) Storage modulus versus temperature plot for PPO/VA (P1) and PPO/VA/polyphosphazenes (P2 and P3). (b) Tan delta versus temperature curve for pure PPO (P), VA, PPO/VA (P1), and PPO/VA/polyphosphazenes (P2 and P3).

PPO/LCP blend. Now in presence of polyphosphazene, PPO/LCP blend exhibits only one glass transition temperature [Fig. 4(b)] suggesting compatibility between the blend partners. The improved compatibility by the addition of compatibilizer may be interpreted as progressive immobilization of the polymer chains close to the boundary between two phases when they were grafted to the compatibilizer phase and the surfactant nature of polyphosphazene. It may be said that the effect of polyphosphazene as a

**TABLE II**  
Variation in Storage Modulus from DMTA Study

Sample code	Storage modulus (MPa)	Storage modulus (MPa) at 100°C (below $T_g$ )
P1	5773	4408
P2	7205	6357
P3	6208	5320

**TABLE III**  
Variation in Tan Delta from DMTA Study

Sample code	Glass transition temperature	
	$T_g^1$ (°C)	$T_g^2$ (°C)
VA	117	–
P1	115	183
P2	166	–
P3	165	–

compatibilizer in varying the glass transition temperature is a reflection of compatibilization extent on the polymer blends. Compatibilization between the polymer blends significantly reduces the domain size of the dispersed phase and/or promotes the chances of fibrillation of TLCP components.

### Heat deflection temperature

The heat deflection temperature (HDT) of the blends is usually affected by particle size, particle size distribution, phase morphology, adhesive force, and residual stress. The effect of polyphosphazene elastomer on HDT of PPO/VA blend has been illustrated in Figure 5. Overall, polyphosphazene-compatible PPO/VA blend exhibits 8–9°C higher HDT than the uncompatibilized PPO/VA blend. Actually in presence of compatibilizer, LCP fibrils are oriented in the direction of flow field, which may cause mechanical reinforcement ensuring improved interfacial adhesion and therefore giving rise to HDT.

### FTIR study

Figure 6 exhibits the FTIR spectra of pure PPO (P), VA, and their respective blends (P1, P2, and P3). FTIR study helps in determining molecular interactions between the blend components. FTIR spectra of pure PPO (Fig. 6) reveal that appearance of two

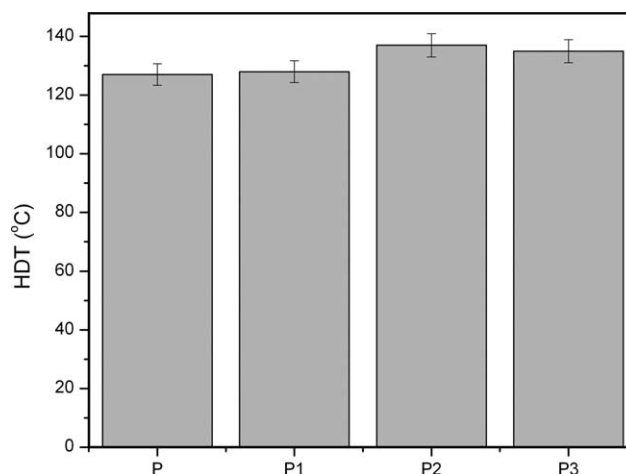


**Figure 5** Comparison of heat deflection temperature of pure PPO (P), PPO/VA (P1), and PPO/VA/polyphosphazenes (P2 and P3).

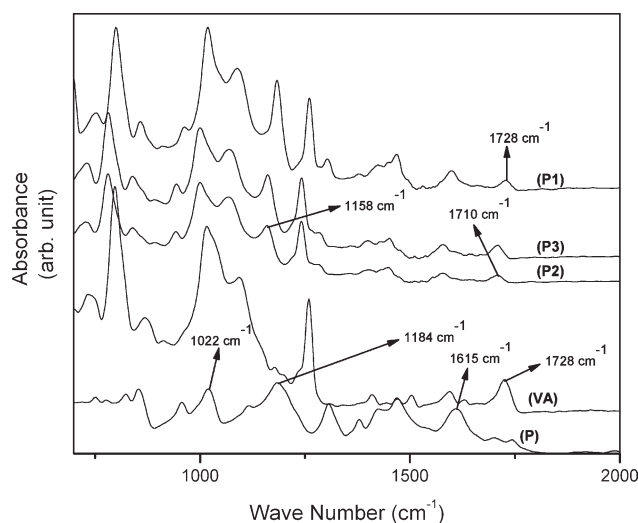


**Figure 6** FTIR plots of pure PPO (P), VA, PPO/VA (P1), and PPO/VA/polyphosphazenes (P2 and P3).

characteristic peaks, one at 1022 and other at 1184  $\text{cm}^{-1}$  corresponding to the C—O stretch. The ring stretching of the PPO gives a band at 1615  $\text{cm}^{-1}$ . Pure LCP shows the characteristic peak at 1728  $\text{cm}^{-1}$  which is probably for C=O stretching. In PPO/VA blend, the peak at 1184  $\text{cm}^{-1}$  become intense in nature suggesting incompatibility between PPO/VA blend system; whereas, the same peak at 1184  $\text{cm}^{-1}$  has shifted to lower frequency region and intensity of the peak gets lowered, i.e., the peak becomes broader in presence of polyphosphazene. Another pertinent observation is that the C=O stretching peak at 1728  $\text{cm}^{-1}$  has shifted to 1710  $\text{cm}^{-1}$  in attendance of polyphosphazene justifying that polyphosphazene plays an important role in changing the chemical environment by reacting with PPO and LCP. Henceforth, the compatibility of the PPO and VA is enhanced via the incorporation of polyphosphazene elastomer.

### XRD study

The XRD pattern has been demonstrated in Figure 7, and the respective data are exhibited in Table IV. It is evident that in presence of LCP some sort of crystalline property is being induced in PPO matrix due to reinforcing properties of LCP. For PPO/VA blend system (P1), two distinct reflections are evident. One at  $d_1 = 4.52 \text{ \AA}$  ( $2\theta = 19.6^\circ$ ) and other at  $d_2 = 3.25 \text{ \AA}$  ( $2\theta = 27.4^\circ$ ), which can be assigned to (110) and (210), respectively.<sup>23</sup> However, in presence of polyphosphazene elastomer, the peak intensity has been found to decrease significantly and also it has been shifted from  $2\theta = 27.4^\circ$  to  $2\theta = 27.0^\circ$ . Moreover, presence of an effective compatibilizer may have an effect in altering the percentage of crystallization, especially in the vicinity of the interface. Ahn et al.<sup>24</sup> reported a reduction in the crystallinity of polyacrylate (Par)/polyamide (PA-6) blends in presence of Par-*b*-PA-6 copolymer. In this study, polyphosphazene elastomer, used as a compatibilizer, plays a role to reduce the percent crystallinity of PPO/VA blend system by reacting at the interface and henceforth forming graft copolymers. Polyphosphazene also increases the mutual solubility of the concerned components, which causes a reduction in the crystallinity of PPO/VA blend system. Therefore, the surfactant nature of polyphosphazene elastomer is vividly justified.

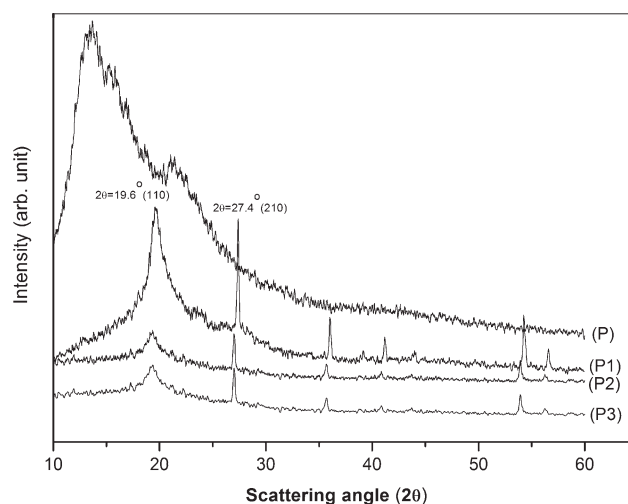


**Figure 7** XRD patterns of pure PPO (P), PPO/VA (P1), and PPO/VA/polyphosphazenes (P2 and P3).

Therefore, the surfactant nature of polyphosphazene elastomer is vividly justified.

### Mechanical property assessment

The morphological differences between blends with and without polyphosphazene elastomer definitely affect their respective physical properties. Variation in tensile modulus, tensile strength, and elongation at break are being displayed in Figure 8(a-c), respectively. The tensile modulus has been found to

**TABLE IV**  
XRD Measurements

Sample code	Peak angle ( $P_1$ , $2\theta$ )	Peak angle ( $P_2$ , $2\theta$ )	Interplaner distance ( $d_1$ ), $\text{\AA}$	Interplaner distance ( $d_2$ ), $\text{\AA}$	% Crystallinity ( $\chi_{c1}$ )
P	13.6	—	6.50	—	14.5
P1	19.6	27.4	4.52	3.25	25.2
P2	19.4	27.0	4.58	3.30	17.4
P3	19.4	27.0	4.58	3.30	17.6

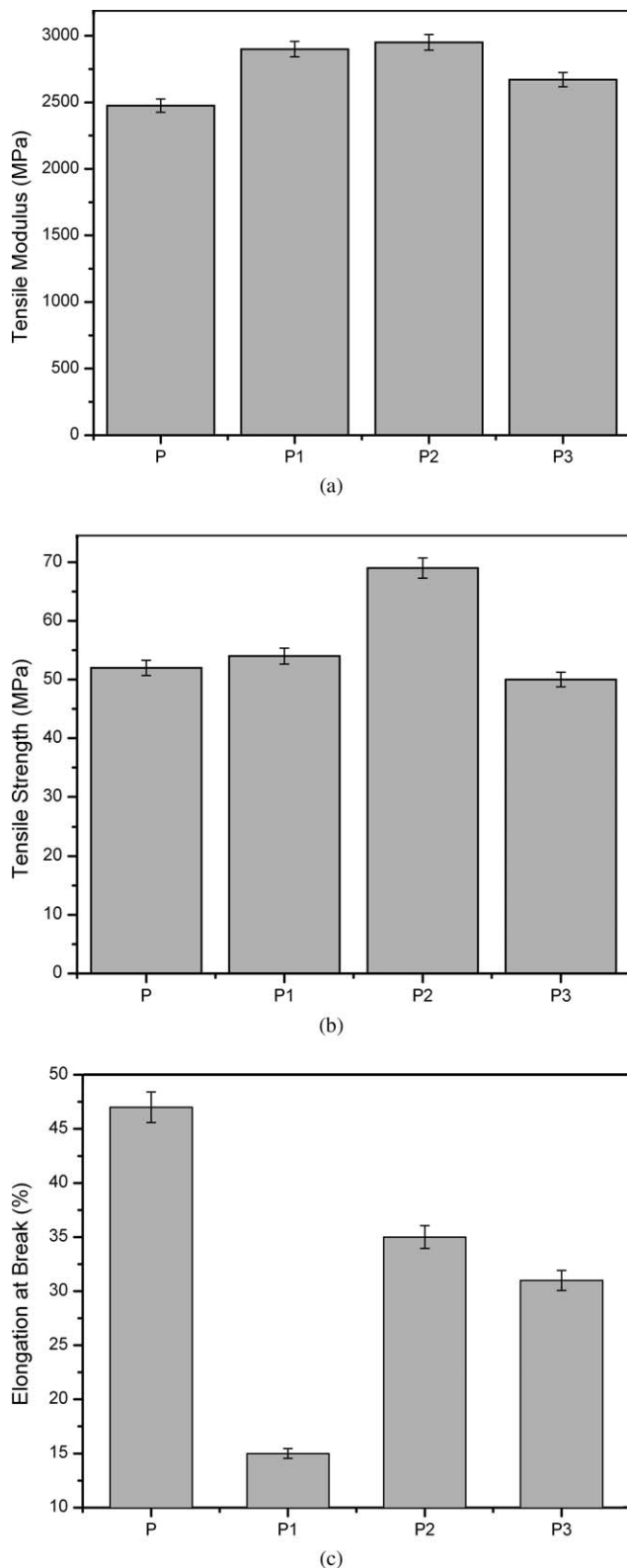


**Figure 8** (a) Variation in tensile modulus in different loading of polyphosphazenes. (b) Variation in tensile strength in different loading of polyphosphazenes. (c) Variation in elongation at break in different loading of polyphosphazenes.

increase with the addition of VA in PPO matrix. However, 2.5 wt % polyphosphazene-compatible ternary blend system does not exhibit a substantial improvement in tensile modulus [Fig. 8(a)], in fact value of modulus reduces in presence of 5 wt % polyphosphazene. The above-mentioned phenomenon may be due to following factors<sup>25</sup>:

1. Polyphosphazene hampering the crystalline-phase development of PPO, and
2. Addition of low-modulus polyphosphazene contributes to the modulus decrease.

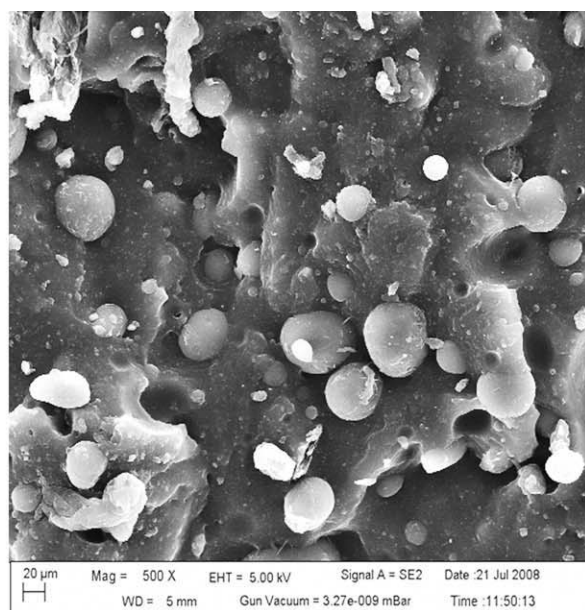
However, the tensile strength shows a significant improvement over that of the binary blend [Fig. 8(b)]. When excess polyphosphazene is added, the inhomogeneity of the structure cause the mechanical properties to deteriorate. The elongation of the 2.5 wt % polyphosphazene-compatible ternary blend is better than that of the binary blend [Fig. 8(c)]. In general, the stiffer the composite, the higher the tensile strength and the lower the elongation.<sup>25</sup> However, our results differ from this expectation. This is ascribable to the role of the compatibilizer. The simultaneous increases in tensile strength (or tensile modulus) and elongation can be explained by improved adhesion due to the compatibilizer at the interface.

### Scanning electronic microscopy

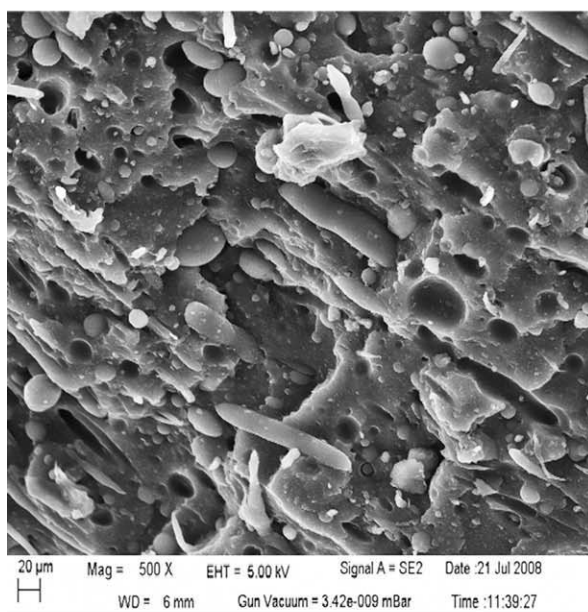
In an effort to provide more support for the compatibility of the ternary blend, the morphologies of binary (PPO/VA) and ternary (PPO/VA/polyphosphazene) blends have been investigated. In the binary blend [Fig. 9(a)] of PPO/VA, the TLCP domains are relatively large because of immiscibility, thereby leading to poor dispersion. The micrographs also demonstrate poor adhesion between the two phases, which leads to an open ring hole around the TLCP domain while TLCP is pulled out during the fracture of the samples. The ternary blend surface [Fig. 9(b)] shows a different morphology. The size of the dispersed phase is noticeably reduced. There is no open ring hole around the TLCP domain, reflecting better adhesion between the two phases. Furthermore, the VA phase shows fibril shapes that are uniformly distributed along the direction of flow. When 5% polyphosphazene is added, a complicated morphology appears [Fig. 9(c)] i.e., TLCP fibril shapes are still observable, but some have been incorporated into large domains. Excess levels of polyphosphazene seem to induce coagulation or flocculation of the dispersed TLCP phase.<sup>26</sup>

### CONCLUSIONS

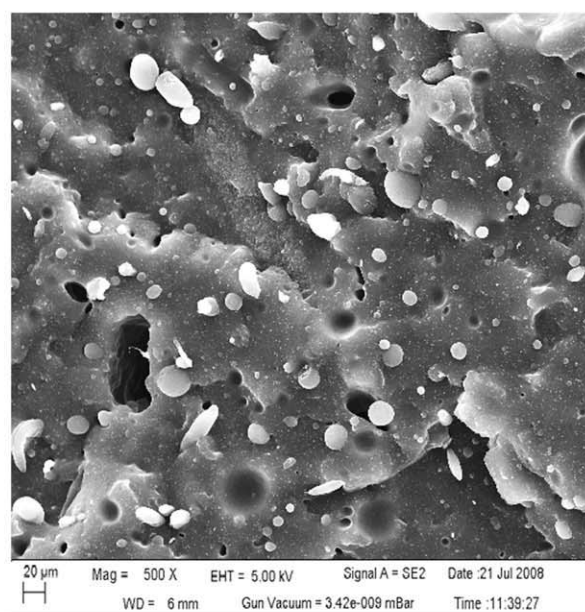
Functionalized polyphosphazene elastomer, acting as a compatibilizer, plays a role in reducing the glass



(a)



(b)



(c)

**Figure 9** (a) SEM micrograph of PPO/VA blend. (b) SEM micrograph of PPO/VA/2.5 wt % polyphosphazenes. (c) SEM micrograph of PPO/VA/5 wt % polyphosphazenes.

transition temperature of the PPO matrix in PPO/VA/polyphosphazene blend system which is evident from DMTA analysis. Thus, surfactant nature of polyphosphazene is vividly justified. A substantial improvement in mechanical properties of the compatibilized blend points towards improved interfacial adhesion. However, in presence of excess polyphosphazene, the in-homogeneity of the structure causes the mechanical properties to deteriorate. SEM observations reveal finer morphology in presence of polyphosphazene. The size of the dispersed

phase is noticeably reduced. There is no open ring hole around the TLCP domain, reflecting better adhesion between the two phases. FTIR study verifies the change in chemical atmosphere in presence of polyphosphazene.

#### References

1. Mantia, F. P. L.; Valenza, A.; Paci, M.; Magagnini, P. L. *J Appl Polym Sci* 1989, 38, 583.
2. Berry, D.; Kenig, S.; Siegmann, A. *Polym Eng Sci* 1991, 31, 451.



3. Klein, N.; Selivansky, D.; Maron, G. *Polym Compos* 1995, 16, 189.
4. Shimizu, H.; Kitano, T.; Nakayama, K. *Mater Lett* 2004, 58, 1277.
5. Limtasiri, T.; Isayev, A. L. *J Appl Polym Sci* 1991, 42, 2923.
6. Turek, D. E.; Simon, G. P. *Polymer* 1993, 34, 2750.
7. Tjong, S. C.; Shen, J. S.; Liu, S. L. *Polym Eng Sci* 1996, 36, 797.
8. Krishnaswamy, R. K.; BinWadud, S. E.; Baird, D. G. *Polymer* 1999, 40, 701.
9. Kohli, A.; Chung, N.; Weiss, R. A. *Polym Eng Sci* 1989, 29, 573.
10. Malik, T. Q.; Carreau, P. J.; Chaplean, N. *Polym Eng Sci* 1989, 29, 600.
11. Croteau, J. F.; Laivins, G. V. *J Appl Polym Sci* 1990, 39, 2377.
12. Meng, Y. Z.; Tjong, S. C. *Polymer* 1998, 39, 99.
13. Zhuang, P.; Kyu, T.; White, J. L. *Polym Eng Sci* 1988, 28, 1095.
14. Bafna, S. S.; Sun, T.; Baird, D. G. *Polymer* 1993, 34, 708.
15. Tjong, S.C. *Mater Sci nd Eng R* 2003, 41, 1.
16. O'Donnell, H. J.; Baird, D. G. *Polymer* 1995, 36, 3113.
17. Zhao, X.; Du, X.; Liu, D.; Zhou, Q. *Macromol Mater Eng* 2000, 274, 36.
18. Chiang, C. R.; Chang, F. C. *Polymer* 1997, 38, 4807.
19. Eklind, H.; Schantz, S.; Maurer, F. H. J.; Jannasch, P.; Wesslen, B. *Macromolecules* 1996, 29, 984.
20. Son, Y.; Lee, S. *Polym Bull* 2006, 56, 267.
21. Cho, C. G.; Kim, S. H.; Park, Y. C.; Kim, H.; Park, J. W. *J Memb Sci* 2008, 308, 96.
22. Xu, T.; Wu, D.; Wu, L. *Prog Polym Sci* 2008, 33, 894.
23. Lee, H. S.; Kim, Y.; Kim, W. N.; Hyun, J. C.; Oh, T. S. *Korean J Rheol* 1994, 6, 96.
24. Ahn, T. O.; Lee, S.; Jeong, H. M.; Lee, S. W. *Polymer* 1996, 37, 3559.
25. Seo, Y.; Kim, B.; Kim, K. U. *Polymer* 1999, 40, 4483.
26. Seo, Y.; Hong, S. M.; Hwang, S. S.; Park, T. S.; Kim, K. U.; Lee, S.; Lee, J. W. *Polymer* 1995, 36, 515.